Chemical Engineering Journal 149 (2009) 370–382

Contents lists available at ScienceDirect

Chemical Engineering Journal

journal homepage: www.elsevier.com/locate/cej

Steady-state and dynamic modeling of commercial bulk polypropylene process of Hypol technology

Zheng-Hong Luo*, Pei-Lin Su, De-Pan Shi, Zu-Wei Zheng

Department of Chemical and Biochemical Engineering, College of Chemistry and Chemical Engineering, Xiamen University, Shiming Street 422, Xiamen 361005, China

ARTICLE INFO

Article history:
Received 15 October 2008
Received in revised form 11 January 2009
Accepted 12 January 2009

Keywords:
Polypropylene
Hypol technology
Polymers Plus
Process simulation
Steady-state and dynamic modeling

ABSTRACT

Both steady-state and dynamic models for the commercial bulk polypropylene process of HYPOL technology were developed by using fundamental chemical engineering principles and advanced software tools, Polymers Plus and Aspen Dynamics. The models consider the important issues of physical property and thermodynamic model selections, catalyst characterization, and reactor model, in addition to the traditional Ziegler–Natta polymerization kinetics. The performance of equilibrium-stage modeling was examined using the perturbed-chain statistical associating fluid theory (PC-SAFT) equation of state and a pre-built reactor model in Polymers Plus. The detection of non-equilibrium behavior for the liquid-phase reactor leads to a novel reactor model suggested in this work, wherein the vapor–liquid equilibrium behavior was separated from polymerization behavior. Besides, the traditional Ziegler–Natta polymerization system was incorporated from single-site to multi-site model by fitting the actual data sourced from open reports and certain plant data. Furthermore, we validated the models using the plant data and demonstrated the application of our dynamic model by simulating a grade change.

1. Introduction

1.1. Scope

Polypropylene is one of the most widespread polymers, and can be produced by various technologies including Hypol technology, Innovene technology, Unipol technology, Catalloy technology, and Spheripol technology, etc. Among them, there are different reactors and/or reactor arrangements in essence [1,3–5]. On the other hand, an accurate and robust polymerization process model can be used in many industrial aspects including process design, optimization, and process control, etc., which results in millions of dollars in cost saving and manufacturing profit increase in industry [3–5].

Generally, an excellent polymerization process model, which describes physical and thermodynamic properties, phase equilibrium, and polymerization kinetics, is vitally useful for exploring changes in feed composition and operation conditions [1]. Physical properties, such as vapor and liquid densities, allow the model to accurately predict the residence time of the reactant in the reactor and the throughput of product. Phase equilibrium is important for modeling the flash vessels in the overhead recycle units and in reactors with multiple phases, where the respective residence time of each phase is related to the phase equilibrium. A robust model must account for these considerations. In addition, although process rate depends on the driving force of the process related to the thermodynamic variables, it must be pointed out that the thermodynamic considerations do not establish the equation of the process rate [2]. As a result, in the process industry, the equilibrium state always transforms toward the thermodynamically advantageous state without indicating whether the flowing materials within the reactor (vessel) reach the thermodynamical equilibrium state or not, or how long they will reach.

Up to now, a number of models have been proposed to describe the olefin polymerization process [1,3–18]. Khare et al. [1] presented a model for the gas-phase polypropylene process using the stirred-bed reactor. Their detailed modeling methodologies, especially the reactor modeling using four continuous stirred-tank reactors (CSTRs) in series, are of great importance to the accurate process simulation of polypropylene. In addition, Khare et al. [3] simulated slurry high-density polyethylene processes. The non-equilibrium behavior in ethylene/polyethylene flash separators was detected in their work. Buchelli et al. [4,5] succeeded in solving this nonequilibrium problem using a complex unit-operation module embedded in the Polymers Plus software. As a whole, there are many methodologies proposed in the literatures, which succeed in developing a comprehensive model for polyolefin processes using the Polymers Plus software. These methodologies include the selection and parameter's tuning of physical properties and thermodynamic model [6–10], catalyst characterization [11–14] and polymer properties [15,16], in addition to the single- and multiple-site of traditional Ziegler–Natta polymerization kinetics [1,3]. However, here we still point out that most of past models

* Corresponding author. Tel.: +86 592 2187190; fax: +86 592 2187231.
E-mail address: luozh@xmu.edu.cn (Z.-H. Luo).

1385-8947/$ – see front matter © 2009 Elsevier B.V. All rights reserved.
doi:10.1016/j.cej.2009.01.021

Nomenclature

a	regressed correlation parameter
A	heat transfer area of the jacket wall in reactor (m^2)
B	regressed correlation parameter
CAT_i	inactive catalyst site of type i
C_p	heat capacity (kJ/kg)
D_n	inactive polymer chain containing n monomer segments
$[D_n]$	concentration of inactive polymer chains containing n monomer segments (mol/L)
DP_n	number average of the polymer degree of polymerization
DP_w	weight average of the polymer degree of polymerization
$DCAT_i$	deactivated catalyst site of type i
$F(r)$	accumulative weight fraction of chains of length r
G_{pp}	flow rate of polypropylene streams (kg/s)
G	flow rate of streams (kg/s)
H	enthalpy of component (kJ/mol)
k_{ij}	binary interaction parameter in the PC-SAFT EOS
$k_{ds,i}$	rate constant for spontaneous deactivation of catalyst site type i (s^{-1})
$k_{ini,i}$	rate constant for active site initiation at site type i (L/mol s)
$k_{p,i}$	rate constant for initiated active site propagation at site type i (L/mol s)
$k_{pa,i}$	rate constant for atactic chain propagation at site type i (L/mol s)
$k_{sp,i}$	rate constant for activation of catalyst site type i (s^{-1})
$k_{th,i}$	rate constant for chain transfer to hydrogen for site type i (L/mol s)
$k_{tm,i}$	rate constant for chain transfer to monomer for site type i (L/mol s)
K	regressed correlation parameter in Eq. (13) or heat transfer efficiency in Eq. (16)
K_B	Boltzmann constant (1.38×10^{-23} J/K)
m	segment number in the PC-SAFT EOS
m_i	mass fraction of polymer produced at site type i
M	molecular weight of monomer
M	monomer component
MI	melt index (g/10 min)
MWD	molecular-weight distribution
M_n	number-average molecular weight (g/mol)
M_w	weight-average molecular weight (g/mol)
n	number of monomer segments in the polymer (degree of polymerization)
n_{st}	number of active site types
P	reactor pressure (MPa)
$[P_n]$	concentration of active polymer chains containing n monomer segments (mol/L)
PDI	polymer polydispersity index
p	propagation probability of a growing live polymer molecule
$P_{0,i}$	activated catalyst site of type i
$P_{1,i}$	initiated catalyst site of type i
$P_{n,i}$	live polymer chain containing n segments attached to catalyst site type i
Q	heat transferred (kJ/s)
R_{pp}	reaction rate of propylene ($kg/L^{-1}\ s^{-1}$)
r	size parameter for polymer species in the PC-SAFT EOS; ratio of the characteristic chain length to the number-average molecular weight (mol/g)
S_c	split fraction of the stream to be cooled
S_e	equilibrium efficiency
S_f	equilibrium factor
T	temperature (°C)
T_0	temperature of the feed flow (°C)
T_c	temperature of the outflow from the flash drum (°C)
T_{in}	temperature of the inflow of liquid propylene (°C)
T_m	the mean temperature between the coolant and reactor wall (°C)
T_{out}	temperature of the outflow from polymerization reactor (°C)
$w_i(n)$	weight fraction of chains of length n produced at catalyst site type i
$W(n)$	total weight fraction of chains containing n segments
$W(r)$	weight fraction of chains of length r
W_s	work done by the stirred shaft (kJ/s)
V_R	reactor volume (m^3)
τ_i	reciprocal of the polymer number-average molecular weight
ε/k	the segment energy parameter in the PC-SAFT EOS (K)
λ_i	ith moment for all polymer chains
μ_i	ith moment for active polymer chains
σ	the segment diameter in the PC-SAFT EOS (Å)
ΔH	heat of vaporization (kJ/mol)
ΔH_R	heat of polymerization (kJ/mol)

were concentrated on the polyethylene process and the gas-phase polypropylene process. Unfortunately, we are not aware of any comprehensive modeling of the commercial bulk polypropylene process of the HYPOL technology in the open literature prior to our current work [17,18].

In this work, we developed both steady-state and dynamic models for the commercial bulk polypropylene process of the HYPOL technology using fundamental chemical engineering principles and advanced software tools, Polymers Plus and Aspen Dynamics. The primary objective of this work is not only to reproduce a similar process simulation for another olefin technology, but also to focus on the thermodynamical understanding and accurate modeling of the polymerization reactors of the Hypol technology with nonequilibrium behavior detected inside, and, moreover, to discuss the limitation of the thermodynamics and suggest the proper efforts that could be paid special attention to during the developing of the process model.

In the following sections, we try to briefly introduce some methodologies used in this work, and most of the efforts are focused on the reactor modeling which is the most complex and important in our simulation due to the nonequilibrium behavior detected and also makes our work significative in the polyolefin process simulation.

1.2. Commercial bulk polypropylene processes of Hypol technology

The Hypol technology is one of the most widespread commercial methods of producing polypropylene. The technology is originally developed by Japanese Mitsui Petrochemical Company. Fig. 1 shows a simplified flowchart for a typical polypropylene process of the Hypol technology from Lanzhou Petrochemical Company of China National Petroleum Corporation (CNPC). The key part of the flowchart constitutes of two liquid-phase CSTRs and a gas-phase fluidized-bed reactor (FBR).

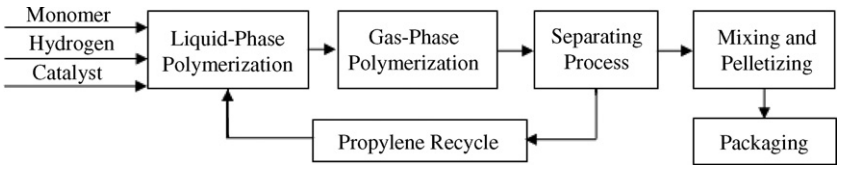

Fig. 1. Production strategy of Hypol technology for polypropylene.

The polymerization firstly carries out in the two liquid-phase CSTRs to form a slurry, then the slurry is flashed and the polymerization continues in the gas-phase FBR. The process uses a titanium-based catalyst and an aluminum-alkyl-based cocatalyst, which are titanium tetrachloride ($TiCl_4$) and triethyl aluminum [$Al(C_2H_5)_3$], respectively in our discussion. Besides, hydrogen entering along with the vapor recycle streams is used as the molecular-weight control agent to produce various grades of polypropylene, and the tacticity control agents fed along with the catalyst are commonly used to increase the isotactic content of the polypropylene.

Fig. 2 gives corresponding polymerization diagram of the Hypol technology using two CSTRs (the liquid-phase polymerization section) and a FBR (the gas-phase polymerization section), which are the heart of the Hypol technology. The reactor temperature ranges from 65 °C to 80 °C, and the pressure ranges from 1.80 MPa to 3.1 MPa. However, there is also a gas-phase within the top of the CSTRs, wherein the vaporization of the liquid monomer removes a large portion of the highly exothermic heat of polymerization. The off-gas from FBR reactor is condensed, flashed, and returned to the two CSTRs.

1.3. Modeling technique

As reported in Refs. [1,3,19], the models integrated the fundamental chemical engineering principles and advanced software tools for both steady-state and dynamic process simulation. The modeling considerations include mass and energy balances, physical properties, phase equilibrium, polymerization kinetics and reactor modeling. We use Polymers Plus and Aspen Dynamics owned by Aspen Tech. Co. to simulate the process.

Polymers Plus [5] is a general-purpose process modeling system for the simulation of polymer manufacturing processes built on top of Aspen Plus as a layered product. By considering a polymer chain as a series of segments whose structures are well-defined, the so-called segment-based approach, Polymers Plus can characterize polymers and can record their structural properties in the whole process. This technique permits the modeling of polymer properties such as molecular weight and copolymer composition and can account for the fact that most polymer products contain an ensemble of molecules having a distribution of chain lengths. Another excellent aspect of Polymers Plus is its special component characterization for Ziegler–Natta catalyst, by which multi-site type of the catalyst can be considered to account for a broad molecular-weight distribution.

After the steady-state process models have been completely set up within Polymers Plus, the models can be exported to Aspen Dynamics to create dynamic models with appropriate control schemes, through which a polymer grade transition can be simulated.

2. Physical and thermodynamic properties

2.1. Introduction

The accurate descriptions of the thermodynamic properties and phase behavior in reactors, separation units, etc., are the most important aspects in the process simulation. Choosing the model with appropriate property for thermodynamic calculations is a challenging work; this is not only because of the large variety of thermodynamic models found in open reports, but also because of the complexity of the polymer systems compared with those of conventional mixtures. There are two categories of thermodynamic models, namely, activity-coefficient category and equation-of-state (EOS) category [8]. In this work, the nature of the species involved and the high pressure conditions in the whole process suggest the use of an equation of state. The polymer which is composed of a large number of segments (repeating units of identical structure) exhibits thermodynamic properties that significantly differ from those of normal molecules. Different property models are required to describe the polymer behavior.

Polymers Plus contains several properties and thermodynamic models of EOS specifically developed for polymer systems. Among them, a model suggested by Gross and Sadowski [6,7] is based on the perturbed-chain statistical associating fluid theory (PC-SAFT) and shows excellent performance in representing the thermodynamic properties of polymer systems. Therefore, the PC-SAFT equation was used to describe the thermodynamic properties of the polymer

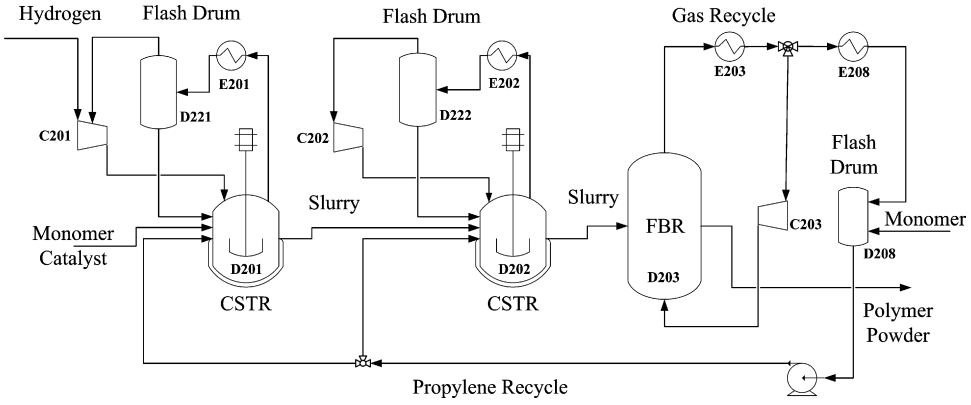

Fig. 2. Schematic flowsheet of the polymerization section of Hypol technology. (C201, C202 and C203: compressor; D201 and D202: liquid-phase polymerization reactor; D203: fluidized-bed reactor; D221, D222 and D208: flash drum; E201, E202, E203 and E208: heat exchanger.)

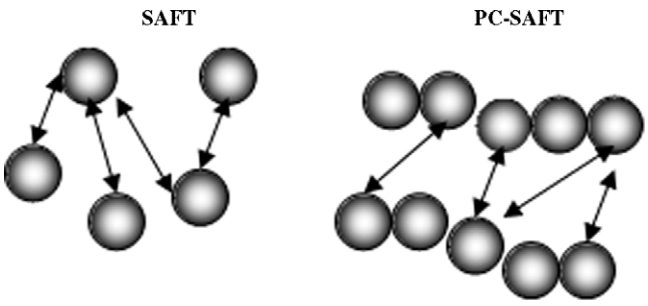

Fig. 3. The difference between SAFT and PC-SAFT equations.

systems in this work, which is the same as other works [1,5,17–20].

In the PC-SAFT equation, Gross and Sadowski [6,7] used the Barker–Henderson second-order perturbation theory of spherical molecules and extended it to chain molecules. The idea is that the concept of the perturbation theory is applied to segments that are connected to chains, other than to disconnected segments which are the case in SAFT, and this difference is clearly showed in Fig. 3. Thus, this improvement has resulted in a more realistic description of the thermodynamic behavior of mixtures of chainlike molecules. For more information on the PC-SAFT equation used in this work, the reader is encouraged to refer to Refs. [1,5–7,17–20]. In this work, all pure-component parameters involved in the process were taken directly from Refs. [1,6,7]. In addition, the applied pure-component parameters for the PC-SAFT EOS are listed in Appendix A.

2.2. Polymer properties

In this study, the polymer properties related to the process can be described as follows.

2.2.1. Molecular-weight distribution

In order to characterize the polymer properties, one must take into account the fact that any polymer is a mixture of components with different chain length. Namely, any polymer has chain length distribution, or molecular-weight distribution (MWD).

For the polymer MWD, a dual approach within Polymers Plus was used, namely, the method of moments for calculating average properties and the method of instantaneous properties for distribution calculation [1,3,15,19].

From the modeling standpoint, many theoretical and empirical functions have been developed to describe the polymer MWD. Flory [21] developed one-parameter equations, which are widely used and known as the most-probable distribution. The corresponding equations are as follows:

$$\text{For the number MWD,} \quad F(r) = p^{r-1}(1-p) \tag{1}$$

$$\text{For the weight MWD,} \quad W(r) = np^{r-1}(1-p)^2 \tag{2}$$

$$p = 1 - \frac{1}{\mathrm{DP}_n} \tag{3}$$

where r is the number of segments, p is the chain-propagation probability of the polymer molecule, DP_n is the number average degree of polymerization of the polymer.

2.2.2. Melt index

Controlling melt index (MI) is an important issue for producing desired grade of polypropylene. Several MI models have been proposed in open literatures. For example, Karol et al. suggested a Quackenbos equation for high-density polyethylene made over chromocene-based catalysts [22,23]:

$$\mathrm{MI} = 1.0 \times 10^{18}(0.2M_w + 0.8M_n)^{-3.9} \tag{4}$$

Sinclair [24] suggested a simple associated equation:

$$\mathrm{MI} = \left(\frac{111525}{M_w}\right)^{\frac{1}{0.288}} \tag{5}$$

Recently, Seavey et al. [25] put forward another associated equation for linear polymers:

$$\frac{1}{\mathrm{MI}} = 3.63 \times 10^{-20}(M_w)^{3.92} \tag{6}$$

However, these equations are highly empirical and often depend on the type of polymer. Nevertheless, within Polymers Plus, MI and other end-use properties are available as user property sets (PropSet), and it allows the specification and direct modification of the add-on user correlations in the form of a FORTRAN subroutine.

3. Reactor modeling

3.1. Introduction

For the process simulation by Polymers Plus and in order to select the proper module in the module library of Polymers Plus, it is necessary and significant to analyze the target unit-operation modules firstly, for example, the polymerization reactors in the heart of the Hypol technology. The upmost principle of these module selection procedures is to represent the actual unit-operation equipment as accurate as possible under the conditions of assumptions and simplifications that are necessary, which, as a result, also helps the whole process simulation to converge efficiently and steadily to a reliable result. However, not all the equipments used in the plants have their corresponding modules provided in Polymers Plus, and still, some special and distinctive equipments are not satisfied with most of the default assumptions and module solution algorithms. So, many of efforts must be made to improve these disadvantages.

In this section, we focus on the modeling of the reactors of the Hypol technology. The nonequilibrium behavior in the liquid polymerization reactors is discussed; accordingly, a complex module is developed based on fundamental chemical engineering principles and modules provided in Polymers Plus. In addition, as to the liquid-phase system, we focus on discussing the modeling for the D201 system in the section. In practice, D201 and D202 are the same liquid-phase CSTRs. Therefore, corresponding module for the D201 system can also be applied to the D202 system.

3.2. Liquid-phase polymerization reactors

3.2.1. Equilibrium-stage approach modeling

Based on the thermodynamic model and component parameters that are suitable to the reaction conditions and components involved in present process, a RCSTR module within Polymers Plus was selected to model the liquid-phase polymerization reactor of D201, wherein no polymer was existed in the feed streams to make it easy for dealing with the input forms. Besides, the characterization of the Ziegler–Natta catalyst and a set of single-site kinetic schemes with reaction rate constants introduced in Section 4 are incorporated into this section. The predicted data and those collected from certain plant are listed in Table 1 for comparison.

The flowsheet for D201 modeling with equilibrium-stage approach is shown in Fig. 4. It is obvious that the model over predicts the residence time of the liquid phase and the mass-flow rate of the slurry streamed out of D201. Namely, most of the liquid propylene fed into the reactor has vaporized in the thermodynamical equilibrium stage. What's more, when the streams of V201A and V201B are combined together, which accords with the spot case of the Hypol technology, the calculation procedure of this flowsheet would generate severe convergence problem.

Table 1
Results of equilibrium-stage approach modeling compared with plant data measured.

Object	Equilibrium-stage approach result	Plant measurement result
Feed rate (kg/h)	11540.059	11540.09
Slurry out rate (kg/h)	9421.718	11537.77
Slurry density (kg/m^3)	668.587	639.858
Polymer produced (kg/h)	5744.775	6142.733
Vapor residence time (h)	0.0123	0.0127
Liquid residence time (h)	1.2490	0.9758

However, it is widely accepted that residence time is one of the important aspects of chemical engineering principles, because it has a great influence on the estimation and applicability of the reaction rate constants based on a certain type of kinetic scheme. In addition, due to the coupling effect of chemical engineering, inversely, the reaction module and the thermophysical properties both play a vital role in the residence time modeling. Thus, the prediction of residence time is one of the important issues that reflected the accuracy of the whole process simulation.

Based on above discussion, it is clear that the assumptions of equilibrium stage and the rigorous thermodynamic-equilibrium algorithm within the pre-built models of Polymers Plus are not suitable to our investigation, and there are other nonequilibrium factors that affected the fluid behavior in the liquid-phase reactors, as discussed in the following.

3.2.2. Thermodynamical and physical mechanism

The liquid-phase polymerization system of D201 consists of a jacketed stirred-tank reactor, an over-head heat-exchanger, a flash drum and a compressor. Taking this polymerization system as a whole, and according to the law of mass conservation and the strategy of steady-state simulation, since there are only liquid streams introduced into this module and also only liquid effluences from this module, the gas propylene came from the vaporization of liquid propylene owing to taking in the polymerization heat should be liquefied, and then exits from this module. In addition, the solid polymer is considered to be a material dissolved in the liquid propylene, which is a usual treatment within Polymers Plus and has been proved to be reasonable and affects the overall vapor–liquid equilibrium [3] to a little extent. Due to the great heat-transfer resistances of the jacket cooling system, mainly the polymer films on the reactor wall [19], a large portion of the highly exothermic heat of polymerization was removed by boiling the liquid propylene. Namely, the propylene acts both as the reactant and the medium of heat exchange.

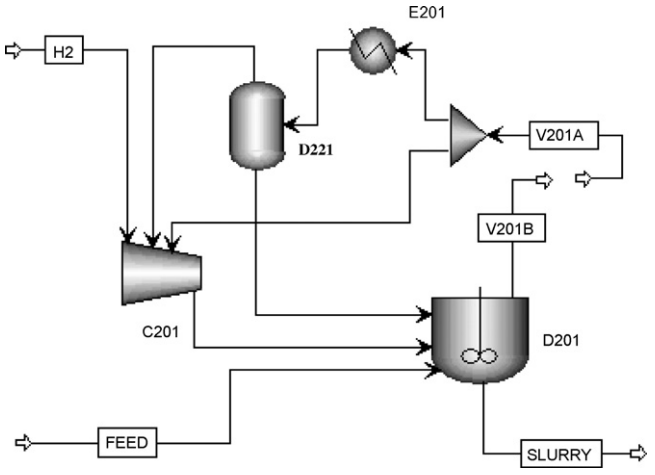

Fig. 4. The equilibrium-stage approach for liquid-phase polymerization system. (C201: compressor; D201: liquid-phase polymerization reactor; D221: flash drum; E201: heat exchanger.)

As shown in Fig. 5, we take the polymerization reactor of D201 as a control volume, streams flowing into and out of the control volume have associated with energies, and all contribute to the energy change of the system. For the sake of simplicity, kinetic- and potential-energy changes in the flowing streams are negligible, the general energy balance of steady-state is obtained [26,27]:

$$\left(\sum_{i=1}^{n} G_i^{\text{out}} H_i^{\text{out}} - \sum_{i=1}^{n} G_i^{\text{in}} H_i^{\text{in}}\right) + \left(\sum_{i=1}^{n} G_i^E H_i^E - \sum_{i=1}^{n} G_i^L H_i^L - \sum_{i=1}^{n} G_i^V H_i^V\right) = \dot{Q}_j + \dot{W}_s \tag{7}$$

$$\sum_{i=1}^{n} G_i^{\text{out}} = \sum_{i=1}^{n} G_i^{\text{in}} \tag{8}$$

$$\sum_{i=1}^{n} G_i^E = \sum_{i=1}^{n} G_i^L + \sum_{i=1}^{n} G_i^V \tag{9}$$

where n represents the number of the components, and H is the enthalpy of each component. Taking the heat capacity, C_p, heat of propylene polymerization, ΔH_R, and the heat of vaporization, ΔH, into consideration; Eq. (9) is rewritten as follows:

$$\sum_{i=1}^{n} G_i^{in} C_P^i (T - T_0) + V_R R_{PP} \Delta H_R + \sum_{i=1}^{n} G_i^E C_p^i (T - T_c) + \sum_{i=1}^{n} G_i^L \Delta H_i = \dot{Q}_j + \dot{W}_s \tag{10}$$

where R_{pp} is the polymerization rate of propylene in the liquid phase which have got V_R in volume. In addition, the heat transferred from the reactor jacket is calculated according to following equation:

$$\dot{Q}_j = -KA(T - T_m) \tag{11}$$

Thus, when D201 is at steady-state, as shown in Eq. (10), the reactor temperature T, and the temperature of the outflow from the

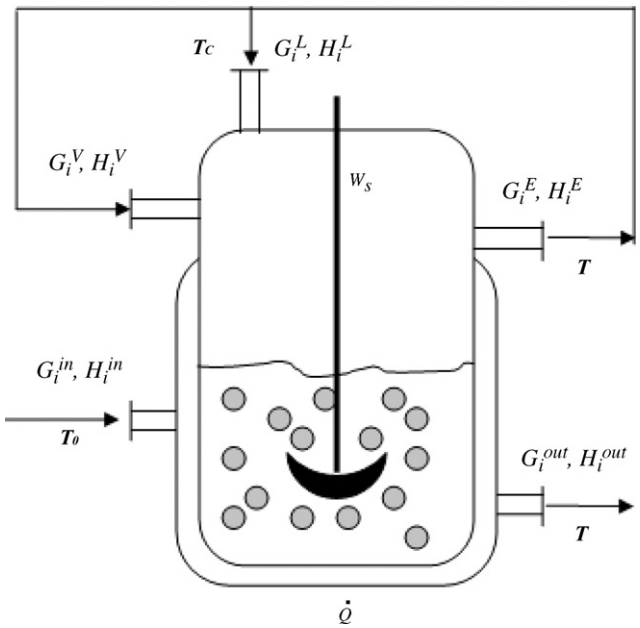

Fig. 5. Energy balance within liquid-phase polymerization reactor.

flash drum, T_c, are constant, as a result, the amount of liquid propylene that vaporized in the reactor during the polymerization and is then re-liquefied in the overhead heat-exchanger, G^L, depends on the polymerization rate in essence.

In other words, the heat released due to the propylene polymerization plays a decisive role in the amount of the vapor vaporized and the vapor–liquid equilibrium in the polymerization reactor, though the limit of this vaporization is the thermodynamical vapor–liquid equilibrium under the conditions of T and P within D201. Hence, the equilibrium-stage approach is not a reasonable assumption for the present study.

3.2.3. Nonequilibrium-stage model

In this work, a nonequilibrium-stage model is designed to settle above problems which are as follows: (1) how much liquid material is vaporized during its residence in polymerization reactor, and (2) how much heat is removed by the over-head heat exchanger, which is, of course, essentially important for the steady-state production of polypropylene.

Aspen FLASH and RCSTR unit operation modules can be used to deal with the equilibrium-stage modeling. Herein, we involve two modules to describe a nonequilibrium-stage module. The Aspen Plus flowsheet for the simplified liquid-phase nonequilibrium polymerization reactor system is shown in Fig. 6. S1 is a splitter and stream 1, the liquid-phase feed stream, is divided into two streams, one of which is stream 2 entering into D201A, a FLASH module, where the materials reach the thermodynamical vapor–liquid equilibrium; the other is stream 3 flowing into D201B, a RCSTR module, wherein the whole material is set as liquid phase only. In the Flash module D201A, the vapor phase of stream 4 at equilibrium stage is partially cooled in a heat exchanger E201 by splitter S2, therefore, a large amount of propylene is liquefied and re-introduced into D201A and D201B through D221 which is a FLASH module with heat duty and pressure both set to be zero to model phase splitting. The rest of the vapors cooled and un-cooled are mixed with hydrogen stream and recycled to D201A. Besides the re-liquefied propylene stream, the equilibrious liquid phase in D201A is redrew into D201B, thus, the total feed stream in liquid phase is introduced completely into D201B where the polymerization proceeds in liquid phase and its slurry output is also in liquid phase. What is more, most of the exothermic heat of polymerization is drawn into D201A to model the heat remove through the propylene boiling.

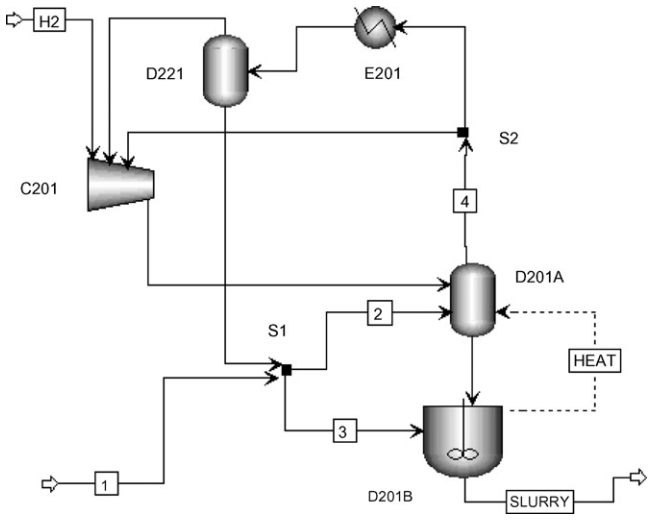

Fig. 6. The nonequilibrium-stage approach for liquid-phase polymerization system. (C201: compressor; D201: liquid-phase polymerization reactor; D221: flash drum; E201: heat exchanger.)

Based on above analysis, D201 is divided into two separate modules, namely, D201A and D201B. D201A functions as a vapor–liquid equilibrium module and D201B focuses on the propylene polymerization reactions, and both are integrated through the heat transferring from D201B to D201A. Then, the split fraction of stream 2 in splitter S1 demonstrates the extent of the real polymerization reactor reaching its thermodynamical vapor–liquid equilibrium.

For hydrogen dissolved in liquid propylene, the complex module suggests that the solubility equilibrium of hydrogen accompanies with the vapor–liquid equilibrium in D201A. However, we also point out that the polymer produced in D201B does not participate in the vapor–liquid equilibrium in D201A. Indeed, a rigorous approach should consider the solubilities of gases that can dissolve in the solid polymer. As discussed previous, the solid polymer is assumed to be dissolved in the liquid phase of propylene, and actually, it is generally considered to be thermodynamically inert. Thus, whether the polymer phase is taken into account within vapor–liquid phase equilibrium or not matters a little in D201A concerning with the boiling of the liquid propylene.

The rest aspects of this section are how to set the configuration of the Aspen Plus modules and how to develop a relation expression for calculating the percentage of the variation of stream 1 to stream 2, which defined as the equilibrium efficiency, S_e. Thus, the higher the equilibrium efficiency is, the more the amount of propylene vaporized under the reactor conditions is.

We set the reactor volume of D201B polymerization reactor as the volume of the condensed phase in the real plant polymerization reactor. Therefore, when the total liquid material enters and exits from D201B reactor with the vaporized propylene in D201A re-introduced as liquid phase, besides, no polymerization reaction conducts on in D201A, hence, the total residence time of the condensed phase is in accordance with the plant reality.

The pressure within D201A should be set in such a way that the pressure in it is a little larger than that within D201B to continue the dynamic simulation.

However, as to the temperature, we decide it on the actual plant data in D201B but not in D201A. Because there is a heat stream introduced into D201A, the pressure specification alone is enough for the FLASH module of Aspen Plus. The built-in equilibrium algorithm will calculate the equilibrium temperature under the feed conditions including the amount of heat introduced in. Obviously, the equilibrium temperature of D201A is largely related to the feed conditions with the heat of the stream being constant.

A design specification of Aspen Plus is needed to make sure that the equilibrium temperature of D201A is equal to that of D201B to make them as a whole reactor theoretically by manipulating the split fraction of stream 2 in S1 splitter module, viz. the equilibrium efficiency. The rest of the modules are specified according to the plant operational conditions.

According to the work of Buchelli et al. [5], the fundamental principles of dimensional analysis are also applied in this study to investigate the relationship between the equilibrium efficiency and the operational parameters. Herein, the equilibrium factor, S_f, is defined from the equilibrium efficiency and described in Eq. (12):

$$S_e = 100(1 - e^{-S_f}) \tag{12}$$

Then, according to the observation in the plant and discussion in Section 3.2.2, we expect that the amount of propylene vaporized is proportional to that of the polymer produced in the outflow stream. And the increase in the flow rate of the feed stream will give rise to the decrease of the residence time and polymer produced, thus the amount of vapor recycling decreases as well. In addition, we have taken into account the temperatures of the liquid stream flowing in and out of the reactor vessel as well as the temperature at the exit of the E201 heat exchanger. Therefore, the final equilibrium factor

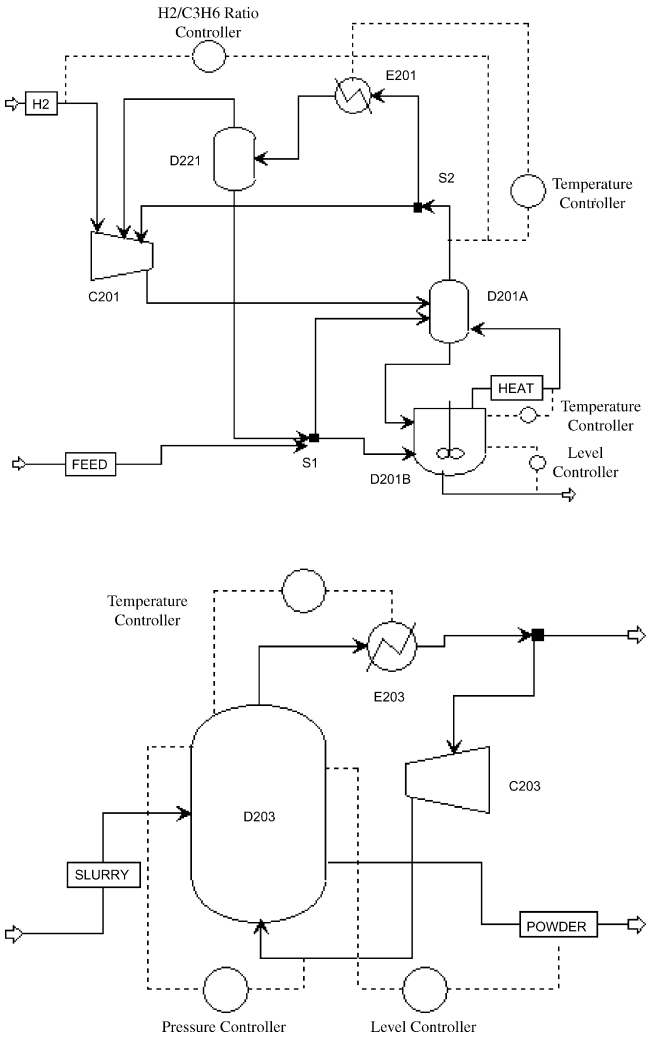

Fig. 7. Conceptual control scheme used to simulate a grade change: (a) liquid-phase polymerization system; (b) gas-phase polymerization system.

is proposed using Eq. (13):

$$S_f = B + KS_c\left(\frac{G_{pp}}{G}\right)^a\left(\frac{T_{in}T_c}{T_{out}^2}\right) \quad (13)$$

where G_{pp} denotes the net production rate of polymer in the reactor of interest, G is referred to the total mass-flow rate of the feed streams, S_c is the split fraction of the cooled portion of stream 4, B, K and a are constants to be determined. Given plant measurements, the unknown coefficients in the above equation can be obtained using a Line-Search method as an optimization of unconstraint multivariable problem. Finally, without going into the mathematical derivation and based on the dimensional analysis, a correlation equation for the equilibrium factor was proposed.

Therefore, the complex unit operation module for liquid-phase polymerization system of D201 were obtained and can also be applied to the second polymerization reactor coded D202. As a whole, the flowsheets for this liquid-phase polymerization system are shown in Fig. 2 and Fig. 7(a).

3.3. Gas-phase polymerization reactor

In the Hypol technology, the gas-phase polymerization reactor D203 is operated as a FBR and is simulated using a RCSTR module within Aspen Plus. The slurry outflow from liquid polymerization system is introduced into the FBR, wherein all the unreacted liquid propylene monomer vaporizes and removes a great deal of the exothermic reaction heat as the polymerization going on in the D203 reactor. Besides, the reaction heat is also removed by the external cooling system, mainly the E203 heat exchanger, which cools the monomer vapor came from the top of D203 and reintroduces the cooled vapor stream into D203 via its bottom by C203 compressor. Thus, in order to maintain the reaction temperature of D203, a design specification of Aspen Plus was involved to manipulate the outlet temperature of E203, while the heat duty of D203 was set to a little amount to meet the plant reality. The flowsheets for this gas-phase polymerization system are shown in Fig. 2 and Fig. 7(b).

4. Polymerization kinetics

4.1. Introduction

The catalyst used in this work is the fourth generation of Ziegler–Natta catalyst, for which polymerization kinetics has been being studied extensively [11–14]. This type of catalyst can produce polyolefins with broad molecular-weight distributions because of its special nature of multiple active site types. In addition, the multisite nature makes the polymerization kinetics complex. A widely accepted set of reaction mechanism and kinetic parameters has not yet been established in open literatures, and reported kinetic parameters often differ from each other. In the Hypol technology, only homopolymer has been manufactured, so only homopolymerization is considered here, and three steps have been put forward in this polymerization kinetics:

(1). Develop a base set of single-site reaction mechanism and kinetic parameters based on the open literatures.
(2). Finely tune the single-site kinetic parameters to match the polymerization rate and DP_n.
(3). Extend the single-site kinetic model to multi-site kinetic model using MWD deconvolution to match polymer polydispersity index (PDI) for several polymer grades.

4.2. Homopolymerization kinetic scheme

In our investigation, we have considered five elementary categories of reaction type as shown in Table 2 according to the open literatures [11–14], which permit the model to access the polymer properties for various grades.

4.2.1. Catalyst activation

To protect the Ziegler–Natta catalyst particles from breaking in the initial polymerization stage, prepolymerization is always adopted in various polypropylene processes. During this procedure, the potential sites on a catalyst tend to be activated quickly by a cocatalyst or spontaneously, considering the constant recipe of the catalyst and cocatalyst, only the spontaneous reaction scheme was hypothetically dealt with and shown in Eq. (14):

$$CAT_i \xrightarrow{k_{sp,i}} P_{0,i} \quad (14)$$

Table 2
Reaction subset used for homopolymerization kinetics.

Reaction number	Description
1	Catalyst site activation
2	Chain initiation
3	Chain propagation
4	Chain transfer
5	Catalyst site deactivation

where $k_{sp,i}$ is the rate constant for activation of catalyst corresponding to the ith site type, and was determined through semibatch reactor experiments to be discussed next.

Within Polymers Plus, a "max sites" parameter was employed to represent the number of catalyst sites per unit mass of catalyst. The utility of the max sites parameter is that it proportionally scales the rates of the reactions involving catalyst sites, permitting us to control the production rate without affecting the molecular weight.

4.2.2. Chain initiation

The activated catalyst sites can be initiated by monomer to form the initiated catalyst site with a single monomer attached

$$P_{0,i}+M \xrightarrow{k_{ini,i}} P_{1,i} \tag{15}$$

where $k_{ini,i}$ is the rate constant at the ith site type. As to the chain initiation, past researchers [1,18,20] always considered the chain initiation as the chain propagation due to absent experimental data. Here it will be discussed.

4.2.3. Chain propagation

Monomer molecules combine with the existing chains at active catalyst sites in succession according to Eq. (16). It leads to the chain propagation

$$P_{n,i}+M \xrightarrow{k_{p,i}} P_{n+1,i} \tag{16}$$

where $k_{p,i}$ is the rate constant of chain propagation at site type i and $P_{n,i}$ and $P_{n+1,i}$ are polymer chains associated with the ith site type of lengths n and $n+1$, respectively.

The chain propagation plays a key role in the adjustment of the polymer molecular weight and appears to be proportionally correlated between them.

To account for the atactic polymer, another propagation reaction is put forward

$$P_{n,i}+M \xrightarrow{k_{pa,i}} P_{n+1,i} \tag{17}$$

where $k_{pa,i}$ is the rate constant of atactic chain propagation at the ith site type, by which the total amount of polymer produced is not affected, and the atactic fraction is described as follows:

$$\text{Atactic fraction} = \frac{\text{rate of atactic propagation}}{\text{rate of total propagation}} \tag{18}$$

4.2.4. Chain transfer

Certain species like hydrogen and monomer may react with a growing polymer chain. It leads to the disengaging of the growing polymer chain from corresponding active site. Accordingly, a dead polymer chain and an empty active site or an initiated active site can be formed. Above process can briefly described below:

$$P_{n,i}+H_2 \xrightarrow{k_{th,i}} D_n+P_{0,i} \tag{19}$$

where $k_{th,i}$ is the rate constant of chain transfer to hydrogen attached to the ith site type and D_n is a dead polymer chain:

$$P_{n,i}+M \xrightarrow{k_{tm,i}} D_n+P_{1,i} \tag{20}$$

where $k_{tm,i}$ is the rate constant for chain transfer to monomer attached to the ith site type. Additionally, it is well agreed that by regulating these two chain transfer rate constants one can realize the modeling target of the number-average molecular weight of the polymer.

4.2.5. Catalyst deactivation

During the polymerization process, the catalyst active site can undergo spontaneous deactivation because of the relative high reaction temperature in catalyst and polymer complex particles. The catalyst deactivations are schematically presented as shown in Eqs. (21) and (22).

$$P_{0,i} \xrightarrow{k_{ds,i}} \text{DCAT}_i \tag{21}$$

$$P_{n,i} \xrightarrow{k_{ds,i}} D_n+\text{DCAT}_i \tag{22}$$

where $k_{ds,i}$ is the rate constant of deactivation for the ith site type, and DCAT_i is a deactivated site for the ith site type. These reactions are seriously taken into consideration to account for the polymer production rate in each series reactor in the period of each time of residence. And this is especially important for the case in which there are three reactors, two are liquid-phase and the rest is gas-phase, encountered in this study.

As the same case for the cocatalyst, we have not included the tacticity control agent due to the constant recipe of the catalyst used during production procedure. However, we assume that it is lumped into above reactions of spontaneous deactivation.

4.3. Determination of kinetic parameters

In this section, we obtain a base set of kinetic parameters originated from the built-in example within Polymers Plus via the methodologies proposed in Refs. [1,3]. To simplify the parameters' determination for highly coupled polymerization kinetics of the Ziegler–Natta catalyst, first, we assume the catalyst contains a single-site type allowing the modeling of the polymerization rate and M_n, but not M_w, or equivalently PDI; second, deconvolute GPC data to confirm the number of the active site types, and determine the relative amount of polymer and the corresponding M_n, produced by each site type. Readers are encouraged to refer to the original literature for detailed discussion, and here, only some important aspects, which have been considered as necessary, are presented below.

4.3.1. Single-site kinetic model

A lot of efforts have been devoted to the polymerization behavior of the patent catalyst used in the present study, thus, instead of using the plant data to tune the kinetic parameters, we first refer to a set of batch experimental data [28] to determine the rate constants of catalyst activation and propagation alone. Using the RBatch module within the Polymers Plus frame, iterative steps have succeeded in fitting this production profile, and Fig. 8 shows that the modeling data agree well with the literature data. The batch experi-

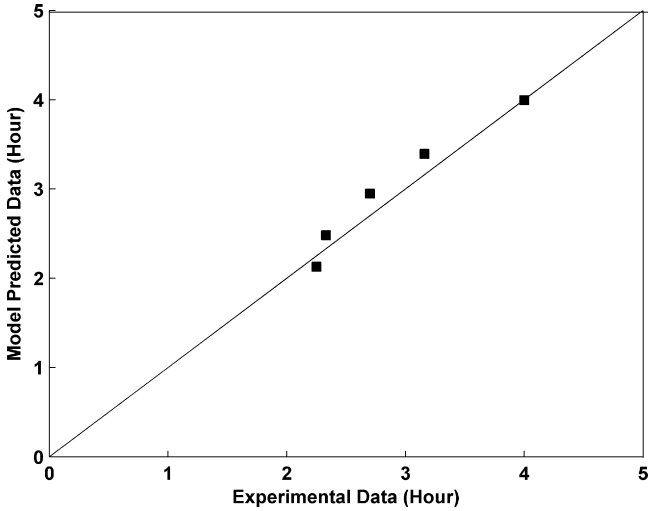

Fig. 8. Fitting results of the single-site kinetic model through batch experimental data.

Table 3
Deconvolution results for a representative polypropylene sample.

Site type	Polymer weight fraction	τ_i	M_n
1	0.0455	4.900×10^{-6}	205,320
2	0.1444	1.400×10^{-5}	71,320
3	0.2766	3.570×10^{-5}	27,990
4	0.3555	8.530×10^{-5}	11,720
5	0.1780	1.949×10^{-4}	5,130

ment was carried out in a batch reactor as a function of the amount of the catalyst under the conditions of constant temperature and pressure, and equal amount of propylene, as a result, different reaction time, at which the same conversion could be measured, was found.

After the accurate residence time is achieved in Section 3 and the polymerization rate agrees well with the batch experimental data, our kinetic parameters' estimation procedure continued, and the attention is focused on the iterative adjustment of the rate constants of chain transfer to hydrogen and monomer.

After several iterative regulations using Aspen Plus design specification, we succeed in modeling both the number-average molecular weight and the polymerization rate in each of the series polymerization reactors, each of which still differ in reaction temperature. Moreover, it is interesting that our single-site kinetic model is suitable for use in both batch and continuous reactor, and both in liquid and gas phases with distinct reaction temperature.

4.3.2. Deconvolution of molecular-weight distribution data

The single-site kinetic model alone is not enough to present most of the polymer properties, especially the MI and PDI. Therefore, it is necessary to establish the number of the active sites through gel-permeation chromatography (GPC) data deconvolution. A simple approach was developed by Soares and Hamielec [16] which proposed a means to extract detailed information of molecular-weight distribution from GPC data.

This algorithm assumed that each site type produces a most-probable MWD,

$$w_i(n) = \tau_i{}^2 n \exp(-\tau_i n) \tag{23}$$

where $w_i(n)$ is the weight fraction of polymer of chain length n produced by each site type i and τ_i is the reverse of the number-average molecular weight of the polymer in site type i. And the chain-length distribution of the composite polymer is the sum of these distributions weighted by the mass fractions of polymer produced at each site type:

$$W(n) = \sum_{i=1}^{j} m_i w_i(n) \tag{24}$$

where $W(n)$ is the total weight fraction of polymer of chain length n; m_i is the mass fraction of polymer produced at each site type, and j is total number of site types. During the deconvolution procedure, j pairs of m_i and τ_i are fitted simultaneously to match the GPC data of plant sample.

Accordingly, the most-probable number of site types was found to be five. Here, one of the representative sets of the results are showed in Fig. 9 and Table 3 in order to prove the value of the most-probable number of site types.

4.3.3. Multi-site kinetic model

Based on above results in Sections 4.3.1 and 4.3.2, we have introduced the multi-site model. It is important to point out that in GPC-deconvolution algorithm m_i represents the polymer weight fraction produced by each site type, instead of the mole or weight fraction of each site type on the catalyst. So, during the transfer from single-site to multi-site model within Polymers Plus, special technique has to be used to apply these GPC-deconvolution results.

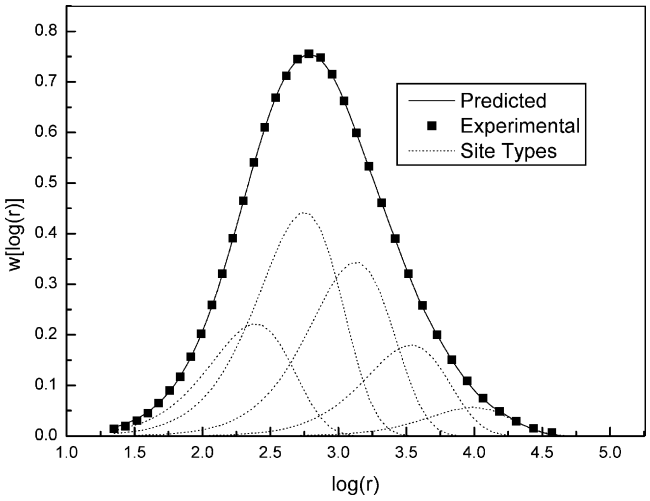

Fig. 9. Deconvolution of a representative MWD results suggesting that a five-site kinetic model is sufficient.

Firstly, we divided the rate constant of catalyst activation for the single-site kinetic model with the number of the catalyst site types, thus an equal number of moles of each site type is achieved.

$$k_{\mathrm{sp},i} = \frac{k_{\mathrm{sp}}}{n_{\mathrm{st}}} \tag{25}$$

where n_{st} is the number of site types considered in the multi-site model. Then, the rate constants of each multi-site reaction were obtained by multiplying the rate constants from the single-site model by the mass fraction of polymer produced at corresponding site type and the number of site types. The equation is shown in Eq. (26):

$$k_{p,i} = n_{st} k_p m_i \tag{26}$$

Next, the efforts are focused on the modeling of the M_n of the polymer produced by each site type. Herein, we adjust the rate constants for chain transfer to hydrogen and to monomer, while still maintaining the same relative contributions of them from the single-site model, thus the sensitivity of these reactions to the concentrations of hydrogen and monomer is not disturbed. We employed the Aspen Plus Calculator and Design Specification module to realize this step of work.

However, above steps of transfer are not adequate to fully and successfully present the polymer PDI or GPC properties because of the highly coupled polymerization mechanism. Some iterative strategies to finely tune the kinetic parameters are necessary in order to meet the targets. For the sake of the limited length of present work, detailed discussion of this section is out of our intention; interested readers are recommended to refer to the original particular literatures [1,3]. In addition, the obtained and applied reaction rate constants for multi-site Ziegler–Natta catalyst are listed in Appendix B.

5. Dynamic modeling

5.1. Introduction

As to dynamic modeling, it has advantage to be able to observe the process response to disturbances or intentionally operational regulation, such as start-up and shut-down or, particularly, grade-change operations which are the most desired in the polyolefin industry.

Benefiting from the Aspen software package, it is convenient to export a steady-state process model from Polymers Plus into Aspen Dynamics with complementary information provided, for instance, vessel dimensions and geometries, to properly account for the delay response to the effect of the process. Moreover, the default PID control schemes are usually configured when the exportation from steady-state to dynamic model is completed. Fine-tunings in PID configuration or even large modifications and additions in the control scheme are necessary in order to perform a more reliable dynamic model.

5.2. Control scheme

As shown in Fig. 7(a), taking the temperature controller of a reactor into consideration, the outlet temperature of E201 heat exchanger was adjusted to maintain the inner temperature of D201A flash module acted as a vapor–liquid equilibrium portion of plant D201 reactor. At the same time a flow controller used to adjust the flow rate of hydrogen to maintain a constant ratio of hydrogen to propylene in the over-head recycle gas was included. Besides, the liquid level of D201B RCSTR acted as a liquid-phase polymerization portion was also accounted by regulating the outlet flow rate.

The control scheme developed for D203 gas-phase reactor (see Fig. 7(b)) involves a temperature controller, which regulates the outlet temperature of E203 heat exchanger to maintain the inner temperature of D203; and a level controller, which controls the output flow rate to keep a steady condensed phase volume; particularly, a pressure controller, which adjusts the amount of vapor recycled to the reactor to maintain its pressure.

6. Simulation results

6.1. Model validation

In our investigation, several sets of data with various operation variables to produce grades of polymer have been used to fit the kinetic parameters. The polymer properties obtained from polymer samples are also incorporated to validate our model. Hence, the application of our present study may be constrained to those close to the operational conditions used in this work.

First, we have performed a procedure of parameters estimation according to our suggestion, namely nonequilibrium-stage approach modeling of the liquid-phase polymerization system, where an Aspen design specification is incorporated to confirm the equilibrium efficiency. Then, with all other inputs specified, Eq. (13) is used in a Line-Search method to obtain the three constant parameters, which are K, B and a. The fitting result is showed in Fig. 10 and it appears to be in good agreement.

Next, the comparisons of simulation results with certain plant data are performed in terms of polypropylene M_n, PDI and MI, The comparisons are shown in Figs. 11–13, respectively. In our investigation, polymer MI is calculated through Eq. (5) with reasonable satisfactions and the model, though its application is limited, matches those polymer properties very well.

6.2. Model application

With most of inputs remained unchanged, our attention was focused on the model sensitivity to certain operationally manipulated variables, such as hydrogen and catalyst feed rate, and the results are showed in Figs. 14 and 15.

Fig. 14 shows that with the increase of the hydrogen feed rate, the polymer MI increases, while the polymer PDI decreases, which is in accordance with our general knowledge of polypropylene manufacturing. And these are useful to approximately confirm the corresponding hydrogen feed rate of certain polymer grade. Catalyst feed rate is usually lowered in the grade-transition process in most operation of olefin plant to reduce the raw material cost and time consumed. In Fig. 15, we analyze the effect of the catalyst feed

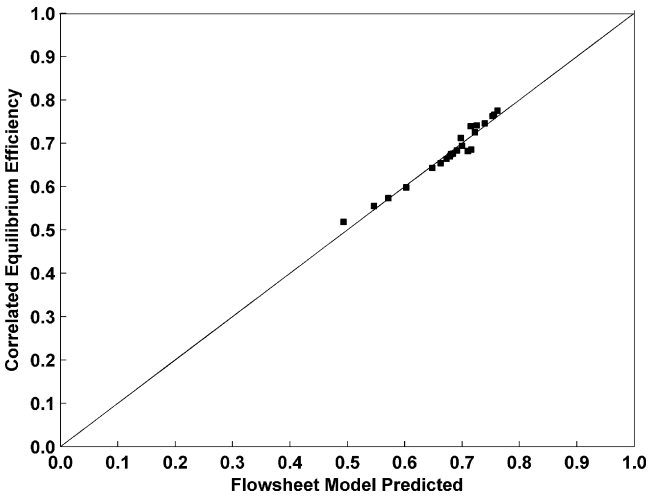

Fig. 10. Fitting result of the nonequilibrium efficiency correlation using model predicted data.

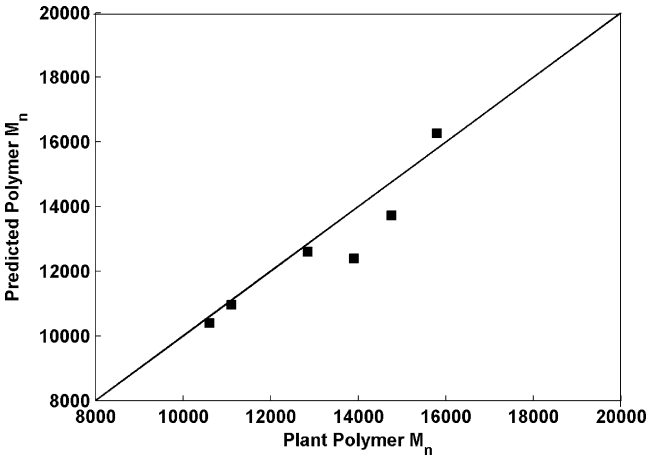

Fig. 11. Comparison of model predictions with plant data for polypropylene M_n.

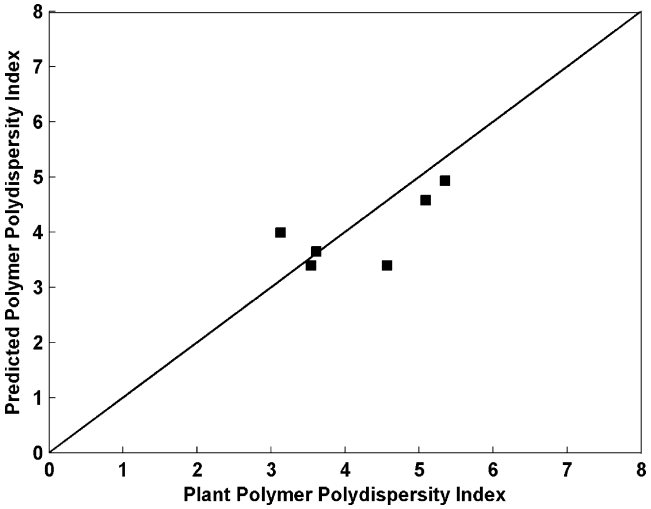

Fig. 12. Comparison of model predictions with plant data for PDI.

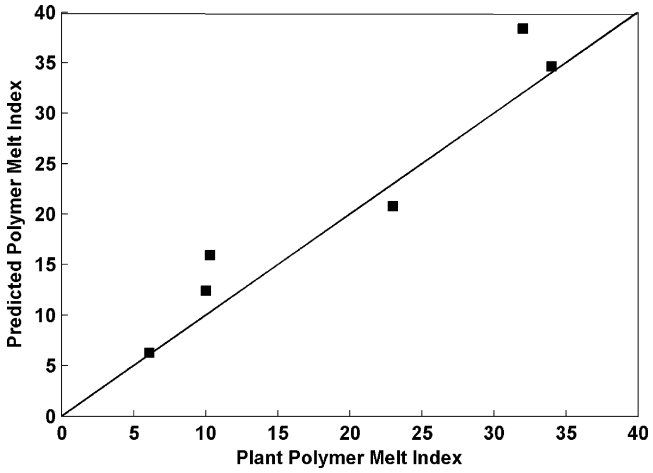

Fig. 13. Comparison of model predictions with plant data for polypropylene MI.

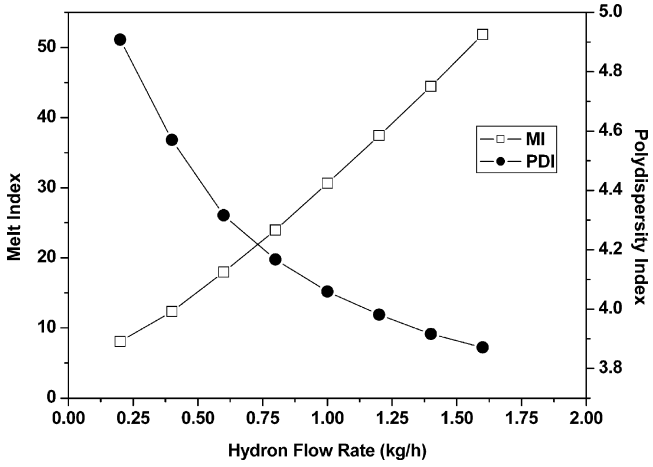

Fig. 14. Sensitivity analysis of the effect of hydrogen flow rate on polypropylene MI and PDI.

rate on the polymer polymerization rate in each polymerization reactor. Whether the possibility of increasing the polymer production rate by increasing the feed rate of catalyst exists, depends on various conditions, for example, heat removing ability in the overhead vapor recycle system, material viscosity within liquid-phase

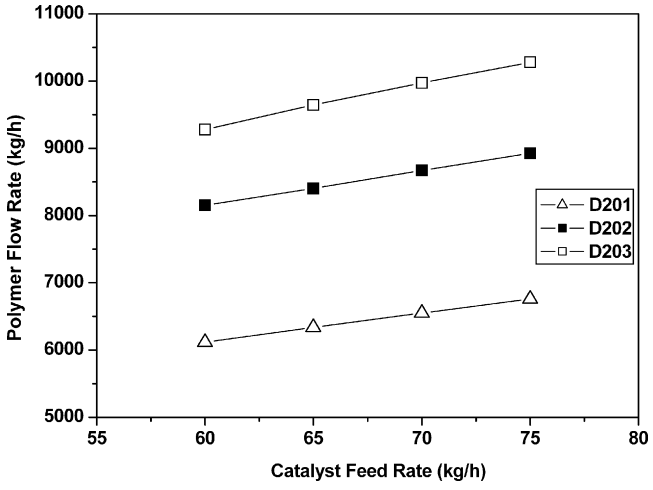

Fig. 15. Sensitivity analysis of the effect of catalyst feed rate on polypropylene production rate in each reactor.

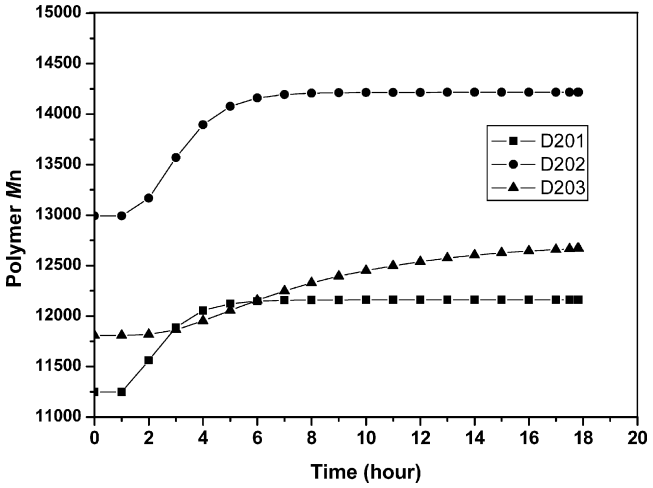

Fig. 16. A polymer grade-transition strategy preformed by a step change in hydrogen flow rate.

reactor, and velocity and pressure drop of the material stream in pipe lines, and so on.

Though the conceptual control schemes have been added to our simulation model, it still differs from the reality of plant operational scenario. A grade-transition operation is performed in our dynamic model, and the results are showed in Fig. 16. It can be observed that with a step increase of the ratio of hydrogen/propylene, the polymer M_n in each reactor steps to a larger stage. And it takes the longest time for D203, which is the last reactor of the polymerization section in the Hypol technology, to achieve steady-state. Besides, due to the lowest reaction temperature and hydrogen solubility in reactor D202, the largest polymer M_n was obtained, which is also in accordance with the reality of plant observation.

7. Conclusions

In this work, we describe the strategy and methodology of modeling for the polypropylene process based on the Hypol Technology. The PC-SAFT equation was used to calculate the thermophysical properties and phase equilibrium of the system, and a nonequilibrium complex module that divides the liquid-phase polymerization reactor into two separate parts, one of which accounts for the vapor–liquid equilibrium wherein the boiling propylene removes the exothermic polymerization heat, the other considers the polymerization procedure in liquid phase. In addition, the polymerization kinetics was established both in the forms of single-site and multi-site models through fitting the batch experimental and plant data. With conceptual control schemes added to the previous steady-state modules, the model system developed in our work can be used to simulate the grade-transfer behavior which is generally in daily production procedure.

Though the present study has been validated, its application or exploration is still limited to similar feed composition and operational parameters. The complex module of liquid-phase polymerization system just makes it more reasonable and reliable for using Polymers Plus, more efforts need to be made to seriously and rigorously account for the whole aspects of this work from chemical reaction engineering, hydrodynamic effects, and chemical thermodynamic issues. However, it is briefly concluded that modeling is a kind of technology of simplifying the complexity while still capturing the essential details.

Table 4
Pure-component parameters for the PC-SAFT EOS.

No.	Component	m	σ (A)	ε/k_B (K)	r (mol/g)	Ref.
1	Hydrogen	0.8285	2.973	12.53	–	[1]
2	Ethylene	1.559	3.434	179.4	–	[1]
3	Ethane	1.607	3.521	191.4	–	[1,6]
4	Propylene	1.960	3.536	207.2	–	[1,6]
5	Propane	2.002	3.618	208.1	–	[1,6]
6	Polypropylene	–	4.147	298.6	0.0253	[1,7]
7	Catalyst	25.0	2.668	198.8	–	[1]
8	Cocatalyst	25.0	2.668	198.8	–	[1]

A sensitivity analysis or heat removing bottleneck can be performed through a detailed simulation model, such as the one proposed in this study. Besides, the grade transition strategies for different span of polymer grades can also be optimized, from which would benefit manufactures a lot.

Acknowledgments

The authors gratefully acknowledge China National Petroleum Corporation, China Lanzhou Petrochemical Company, China Lanzhou Petrochemical Company Research Institute (particularly Zhao, X.T., the Senior President; Zhu, B.C., the Senior Associate President), and Dalian Nationalities University (particularly Dr. Li, B.H.) for supporting this work. We would also like to thank Dr. Liu, Y.A. (Department of Chemical Engineering, Virginia Polytechnic Institute and State University) for his valuable discussion in this work. Authors also thank the anonymous referees for comments on this manuscript.

The simulation work is implemented by advanced software tools (Polymers Plus and Aspen Dynamics) provided by China Lanzhou Petrochemical Company Research Institute and Dalian Nationalities University.

Appendix A. Pure-component parameters for the PC-SAFT EOS

The pure-component parameters for the PC-SAFT EOS are listed in Table 4.

Appendix B. Reaction rate constants for multi-site Ziegler–Natta catalyst

The obtained and applied reaction rate constants for multi-site Ziegler–Natta catalyst are listed in Table 5.

Table 5
Reaction rate constants for multi-site Ziegler–Natta catalyst.

Reaction	Site no.	Comp1	Comp2	Pre-exp	Act-energy (Kcal/mol)	Order	Ref. temperature (°C)
ACT-SPON	1	CAT	–	9.22E−06	7.64	1	69
ACT-SPON	2	CAT	–	9.22E−06	7.64	1	69
ACT-SPON	3	CAT	–	9.22E−06	7.64	1	69
ACT-SPON	4	CAT	–	9.22E−06	7.64	1	69
ACT-SPON	5	CAT	–	9.22E−06	7.64	1	69
CHAIN-INI	1	C3H6	–	22.8849	7.2	1	69
CHAIN-INI	2	C3H6	–	54.9329	7.2	1	69
CHAIN-INI	3	C3H6	–	70.7062	7.2	1	69
CHAIN-INI	4	C3H6	–	208.608	7.2	1	69
CHAIN-INI	5	C3H6	–	98.6969	7.2	1	69
PROPAGATION	1	C3H6	C3H6	22.8849	7.2	1	69
PROPAGATION	2	C3H6	C3H6	54.9329	7.2	1	69
PROPAGATION	3	C3H6	C3H6	70.7062	7.2	1	69
PROPAGATION	4	C3H6	C3H6	208.6084	7.2	1	69
PROPAGATION	5	C3H6	C3H6	98.6969	7.2	1	69
CHAT-MON	1	C3H6	C3H6	0.0865	65.42	1	69
CHAT-MON	2	C3H6	C3H6	0.2171	65.42	1	69
CHAT-MON	3	C3H6	C3H6	0.2308	65.42	1	69
CHAT-MON	4	C3H6	C3H6	0.2535	65.42	1	69
CHAT-MON	5	C3H6	C3H6	0.0462	65.42	1	69
CHAT-H2	1	C3H6	H2	3.0021	10.7	0.5	69
CHAT-H2	2	C3H6	H2	7.5392	10.7	0.5	69
CHAT-H2	3	C3H6	H2	8.0158	10.7	0.5	69
CHAT-H2	4	C3H6	H2	8.7917	10.7	0.5	69
CHAT-H2	5	C3H6	H2	1.6055	10.7	0.5	69
DEACT-SPON	1	–	–	3.4E−4	1	1	69
DEACT-SPON	2	–	–	3.4E−4	1	1	69
DEACT-SPON	3	–	–	3.4E−4	1	1	69
DEACT-SPON	4	–	–	3.4E−4	1	1	69
DEACT-SPON	5	–	–	3.4E−4	1	1	69
ATACT-PROP	1	C3H6	C3H6	0.7251	7.2	1	69
ATACT-PROP	2	C3H6	C3H6	1.7405	7.2	1	69
ATACT-PROP	3	C3H6	C3H6	2.2403	7.2	1	69
ATACT-PROP	4	C3H6	C3H6	6.6097	7.2	1	69
ATACT-PROP	5	C3H6	C3H6	3.1272	7.2	1	69

References

[1] N.P. Khare, B. Luca, K.C. Seavey, Y.A. Liu, Steady-state and dynamic modeling of gas-phase polypropylene processes using stirred-bed reactors, Ind. Eng. Chem. Res. 43 (2004) 884–900.

[2] J.M. Smith, H.C. Van Ness, M.M. Abbott, Introduction to Chemical Engineering Thermodynamic, 6th ed., McGraw-Hill Science/Engineering/Math, 2000.

[3] N.P. Khare, K.C. Seavey, Y.A. Liu, S. Ramanathan, S. Lingard, C.C. Chen, Steady-state and dynamic modeling of commercial slurry high-density polyethylene (HDPE) processes, Ind. Eng. Chem. Res. 41 (2002) 5601–5618.

[4] A. Buchelli, M.L. Call, A.L. Brown, C.P. Bokis, S. Ramanathan, J.A. Franjione, Comparison of thermodynamic equilibrium versus nonequilibrium behavior in ethylene/polyethylene flash separators, in: Presented at the Aspen Technology Users Group Meeting, Houston, TX, February 4–7, 2001.

[5] A. Buchelli, M.L. Call, A.L. Brown, Nonequilibrium behavior in ethylene/polyethylene flash separators, Ind. Eng. Chem. Res. 43 (2004) 1768–1778.

[6] J. Gross, G. Sadowski, Perturbed-chain SAFT: an equation of state based on a perturbation theory for chain molecules, Ind. Eng. Chem. Res. 40 (2001) 1244–1342.

[7] J. Gross, G. Sadowski, Modeling polymer systems using the perturbed-chain statistical associating fluid theory equation of state, Ind. Eng. Chem. Res. 41 (2002) 1084–1093.

[8] H. Orbey, C.P. Bokis, C.C. Chen, Polymer-solvent vapor–liquid equilibrium: equation of state versus activity coefficient models, Ind. Eng. Chem. Res. 37 (1998) 1567–1578.

[9] H. Shen, X.P. Gu, L.F. Feng, Z.W. Tang, B. Liu, Modeling of phase equilibrium in ethylene polymerization system, Chin. J. Proc. Eng. 6 (6) (2006) 626–633 (in Chinese).

[10] L.F. Feng, F.Y. Li, X.P. Gu, Z.W. Tang, B. Liu, Thermodynamic property simulation of propylene–hydrogen-polypropylene system using PC-SAFT equation of state, Petrochem. Technol. 34 (2005) 152–156 (in Chinese).

[11] K.Y. Choi, W.H. Ray, The dynamic behavior of continuous stirred-bed reactors for the solid catalyzed gas phase polymerization of propylene, Chem. Eng. Sci. 43 (1988) 2587–2599.

[12] M. Caracotsios, Theoretical modeling of Amoco's gas-phase horizontal stirred bed reactor for the manufacturing of polypropylene resins, Chem. Eng. Sci. 47 (1992) 2591–2596.

[13] J.J. Zacca, J.A. Debling, W.H. Ray, Reactor residence time distribution effects on the multistage polymerization of olefins. I. Basic principles and illustrative examples, polypropylene, Chem. Eng. Sci. 51 (1996) 4859–4868.

[14] Y.V. Kissin, Multicenter nature of titanium-based Ziegler–Natta catalysts: comparison of ethylene and propylene polymerization reactions, J. Polym. Sci. Polym. Chem. 41 (2003) 1745–1754.

[15] D.J. Arriola, Modeling of addition polymerization system. Ph.D. Dissertation, University of Wisconsin, Madison, WI, 1989.

[16] J.B.P. Soares, A.E. Hamielec, Deconvolution of chain-length distribution of linear polymers made by multiple-site-type catalyst, Polymer 36 (1995) 2257–2264.

[17] J.B. Zhao, P.S. Yang, The simulation of flow apply for polypropylene equipment, Comput. Appl. Chem. 21 (3) (2004) 469–472 (in Chinese).

[18] L.F. Feng, F.Y. Li, X.P. Gu, J.J. Wang, Z.W. Tang, B. Liu, Steady-state modeling of commercial liquid phase bulk polypropylene process with Polymers Plus, Petrochem. Technol. 34 (2005) 237–241 (in Chinese).

[19] C.P. Bokis, S. Ramanathan, J. Franjione, A. Buchelli, M.L. Call, A.L. Brown, Physical properties, reactor modeling, and polymerization kinetics in the low-density polyethylene tubular reactor process, Ind. Eng. Chem. Res. 41 (2002) 1017–1030.

[20] C. Lu, M.H. Zhang, S.J. Jiang, D.Z. Song, Application of Aspen Plus in large-scale polypropylene plant, QILU Petrochem. Technol. 34 (4) (2006) 404–409 (in Chinese).

[21] P.J. Flory, Molecular size distribution in linear condensation polymers, J. Am. Chem. Soc. 58 (1936) 1877–1884.

[22] F.J. Karol, G.L. Brown, J.M. Davison, Chromocene-based catalysts for ethylene polymerization: kinetic parameters, J. Polym. Sci. Polym. Chem. 11 (1973) 413–424.

[23] H.M. Quackenbos, Practical use of intrinsic viscosity for polyethylene, J. Appl. Polym. Sci. 13 (1969) 341–351.

[24] K.B. Sinclair, Characteristic of linear LPPE and description of UCC gas phase process. Process Economics Report, SRI International, Menlo Park, CA, 1983.

[25] K.V. Seavey, Y.A. Liu, N.P. Khare, Quantifying relationships among the molecular weight distribution, non-Newtonian shear viscosity, and melt index for linear polymers, Ind. Eng. Chem. Res. 42 (2003) 5354–5362.

[26] Q.P. Chen, H.S. Wang, W.D. Song, Simulation of continuous stirred tang reactor for polymerization of propene. I. Steady-state simulation of reactor, Chem. React. Eng. Technol. 10 (1) (1994) 33–40 (in Chinese).

[27] Q.P. Chen, H.S. Wang, W.D. Song, Simulation of continuous stirred tang reactor for polymerization of propene. II. Dynamic simulation of reactor, Chem. React. Eng. Technol. 10 (1) (1994) 41–46 (in Chinese).

[28] A.W. Zhou, D. Xie, Discussion on liquid phase bulk polymerization of propylene by using CS-1 catalyst with high efficiency, Petroleum Process. Petrochem. 26 (8) (1995) 32–36 (in Chinese).